Electronic Supplementary Material (ESI) for Journal of Materials Chemistry A.

Supporting Information

Metal organic frameworks-derived hollow cactus-like carbon sheet for oxygen reduction

Ming Zhang, Chaohai Wang, Xin Yan, Klu Prosper Kwame, Saisai Chen, Chengming Xiao, Junwen Qi, Xiuyun Sun, Lianjun Wang, Jiansheng Li*

Jiangsu Key Laboratory of Chemical Pollution Control and Resources Reuse, School of Environmental and Biological Engineering, Nanjing University of Science and Technology, Nanjing 210094, People's Republic of China

lijsh@njust.edu.cn.

Materials and Methods:

Materials:

2-methylimidazole (2-MeIm), $Co(NO_3)_3 \cdot 6H_2O$, $Zn(NO_3)_3 \cdot 6H_2O$, dopamine hydrochloride (PDA), potassium hydroxide (KOH) and nafion were purchased from Sigma-Aldrich. Anhydrous ethanol and sulfuric acid (H_2SO_4) were obtained from Nanjing Chemical Reagent Co., Ltd. All the reagents were directly used without further purification. Deionized (DI) water was used all the experiments.

Synthesis of leaf-like ZIFs. In a typical experiment, 5.0 g of 2-MeIm was added to 100 mL of DI water with stirring for 10 min. Then 1.32 g of $Zn(NO_3)_2 \cdot 6H_2O$ and 0.33 of $Co(NO_3)_2 \cdot 6H_2O$ dissolved in 100 mL solution was added into the above solution with stirring for 3 h at room temperature. The resultant purple precipitate was collected by centrifugation with 3000 r/min for 5 min and washed with DI water and ethanol for three times, respectively. Finally, the purple powder was dried under vacuum 6 h at 80 ˚C.

Synthesis of ZIFs@PDA. In a typical synthesis. 5.0 g of 2-MeIm was added to 100 mL of DI water with stirring for 10 min. Then 1.32 g of $Zn(NO_3)_2 \cdot 6H_2O$ and 0.33 of $Co(NO_3)_2 \cdot 6H_2O$ dissolved in 100 mL solution was added into the above solution with stirring for 3 h at room temperature. 0.25 g of PDA dissolved in 20 mL of DI water was added into above solution for another 8 h at room temperature. The resultant black precipitate was collected by centrifugation with 2000 r/min for 5 min and washed with DI water and ethanol for three times, respectively. After drying, composite ZIFs@PDA was obtained. The composites 0.5-ZIFs@PDA and 0.75-ZIFs@PDA were obtained using the same method except PDA was 0.5 and 0.75 g, respectively.

Synthesis of ZIFs-9, 0.25/0.75-CS/CNTs-9 and 0.5-CS/CNTs-7/8/9/10. 0.5-CS/CNTs-7/8/9/10 were prepared by directly carbonizing 0.5-ZIFs@PDA precursor in N_2 atmosphere at different temperature 700, 800, 900 and 1000 ˚C, respectively. ZIFs-9 and 0.25/0.75-CS/CNTs-9 were obtained by carbonizing the corresponding precursors in N_2 atmosphere at 900 ˚C. The resultant samples were acid etching for 24 h to remove the unstable cobalt nanoparticles.

Characterization: The structure and morphology of samples were confirmed by TEM (FEI T20), STEM (Tecnai G2 F30 S-TWIN), SEM (FEI 250 and JEOL 7800). The composition was investigated by XRD (BRUKER D8, Cu Kα) at 40 kV and 40 mA (λ = 1.5418Å). The N_2 adsorption and desorption isotherms were obtained from Micromeritics ASAP-2020

instrument. X-ray photoelectron spectroscopy (XPS) spectra were obtained by using a PHI Quantera II ESCA System with Al Kα radiation at 1486.8V. Raman spectroscopy was conducted at Renishaw in Via reflex spectrometer system. Thermal investigations are studied by thermogravimetric analysis (TGA, SDT Q600, USA) from 25 to 900 ˚C under Ar with a heating rate of 10 ˚C/min. GC-MS experiments were conducted on an Agilent Technologies 7980 GC equipped with 5975 MS. The chromatographic separations were conducted using an HP-5 MS capillary column (30 m × 0.25 mm. i. d. × 0.25μm).

Electrochemical Measurement. The electrochemical measurement of ZIFs-9, 0.25/0.75-CS/CNTs-9, 0.5-CS/CNTs-7/8/9/10 and Pt/C for ORR were carried out in a three-electrode cell (CHI 760E, CH Instrument, Shanghai). The Ag/AgCl electrode (3 M KCl), platinum sheet and sample-modified glassy carbon were the reference, counter electrode and working electrode, respectively. The working electrode was prepared according to previous literature. 10 mg of catalyst was dispersed in 2 mL of mixed solution of ethanol/water (70/30) and ultrasonic dispersion for 15 min. Then the rotary disk electrode (diameter 5 mm) was covered with 75 μL of catalyst dispersion. After drying, 7.5 μL of nafion solution (10% in ethanol) as the binder was dripped on the surface of catalyst. Finally, the prepared electrode was dried at 50˚C for 3 h. Cyclic voltammetry (CV) tests were measured from 0.1 to 1.1 V versus reversible hydrogen electrode (RHE) in N_2/O_2-saturated 0.1 M KOH aqueous solution (the scan rate: 10 mV s^{-1}). Linear sweep voltammogram (LSV) tests were carried out under different rotations in a N_2/O_2-saturated 0.1 M KOH electrolyte (scan rate: 10 mV s^{-1}). Current–time (*I–t*) tests were performed at the rotation rate of 1600 rpm in a 0.1 M KOH aqueous solution. electrochemical impedance spectroscopy (EIS) were measured in the frequency range of 0.01−100 0000 Hz with 5 mV alternating current amplitude.

The electron transfer numbers (*n*) were obtained according to the Koutecky–Levich (*K–L*) equation, as follows:

$$\frac{1}{j} = \frac{1}{j_k} + \frac{1}{B\omega^{1/2}} \qquad (1)$$

$$n = \frac{B}{0.2F(D_0)^{2/3}(V)^{-1/6}C_0} \quad (2)$$

$$j_k = nFkC_0 \quad (3)$$

where j and j_k correspond to measured and kinetic-limited current densities, respectively; B can be determined from the slope of the K-L plots; ω is the rotation rate (rpm); F is the Faraday constant (96485 C mol^{-1}); D_0 is the diffusion coefficient of oxygen (1.9×10^{-5} cm^2 s^{-1}, 0.1 M KOH); V is the kinematic viscosity of the electrolyte (0.01 cm s^{-1}, 0.1 M KOH); C_o is the concentration of oxygen (1.22×10^{-6} mol cm^{-3}).

The rotating ring-disk electrode (RRDE) cures at 1600 rpm with a scan rate of 10 mV s^{-1}, and the hydrogen peroxide yield (%H_2O_2) is calculated by the following equation:

$$\%H_2O_2 = 200\frac{I_r/N}{I_d + I_r/N}$$

where I_d and I_r are the disk and ring current, respectively. N is the ring current collection efficiency which is determined to be about 0.35 in a 10 mM $K_3[Fe(CN)_6]$ and 0.1 M KNO_3 solution.

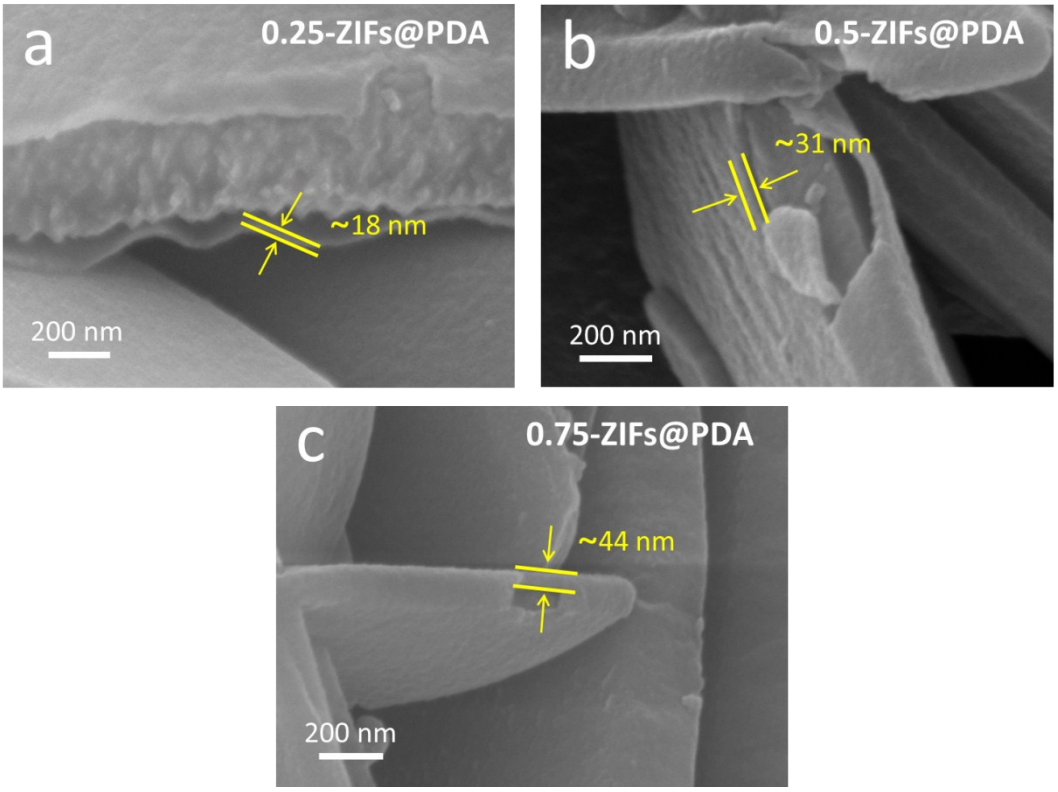

Fig. S1 The thickness of PDA layer for 0.25/0.5/0.75-ZIFs@PDA.

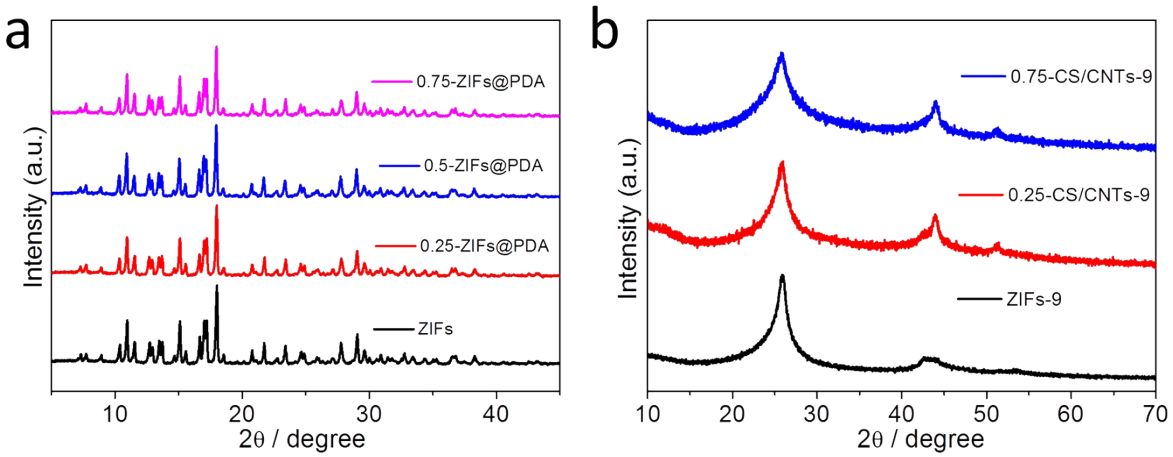

Fig. S2 (a) the powder XRD of precursors ZIFs, 0.25/0.5/0.75-ZIFs@PDA; (b) the powder XRD of carbides ZIFs-9, 0.25/0.75-CS/CNTs-9.

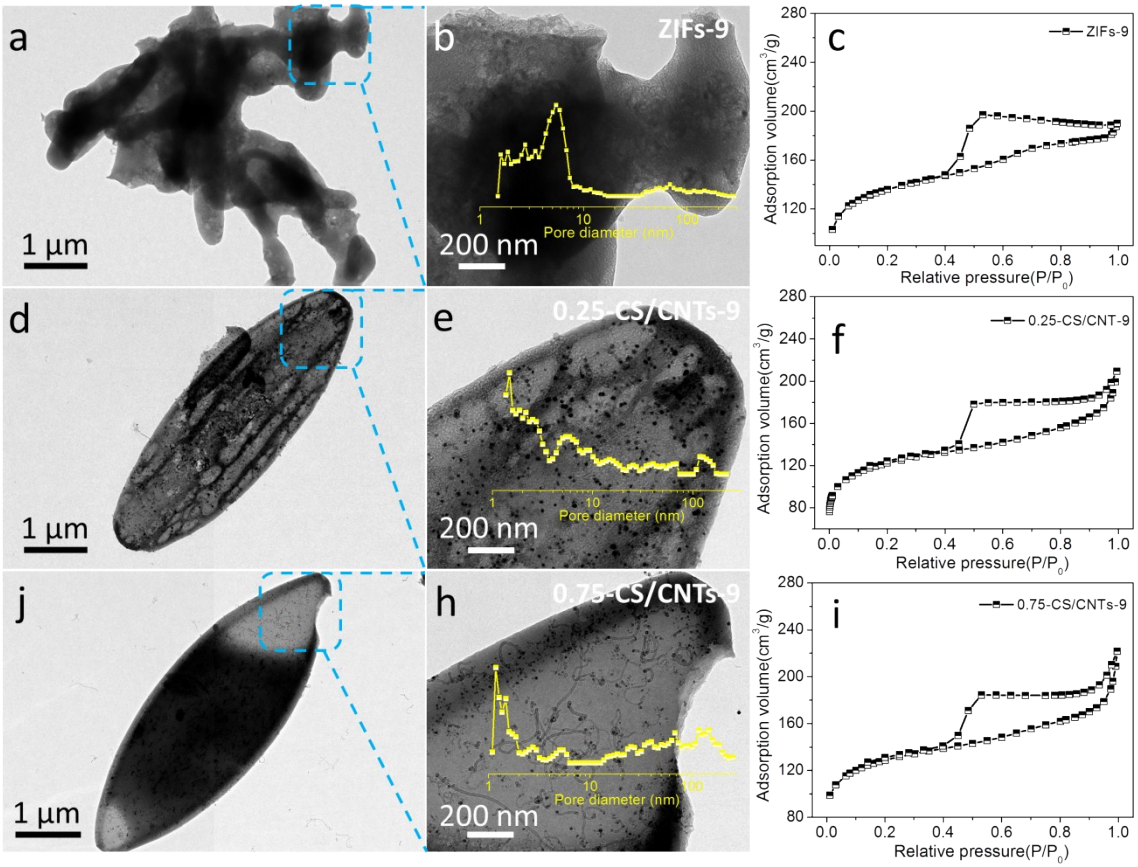

Fig. S3 The TEM (a, d and j), enlarged TEM (b, e and h) images, pore size distribution (inset b, e and h) and N_2-adsorption and desorption curves (c, f and i) of ZIFs-9, 0.25-CS/CNTs-9 and 0.75-CS/CNTs-9, respectively.

Table S1 The S_{BET}, V_{pore}, V_{micro} and the content of different nitrogen species

Sample	S_{BET} (m^2g^{-1})	V_{pore} (cm^3g^{-1})	V_{micro} (cm^3g^{-1})	*All nitrogen* (%)	*Pyridinic-N* (%)	*Pyrrolic-*N (%)	*Graphitic-N* (%)
ZIFs-9	472	0.28	0.12	4.68	26.6	18.2	55.1
0.25-CS/CNT-9	426	0.30	0.10	5.02	31.1	19.8	49.1
0.50-CS/CNT-9	476	0.34	0.11	5.51	33.4	18.4	48.1
0.75-CS/CNT-9	448	0.32	0.11	6.48	31.9	20.3	47.8
0.50-CS/CNT-7	266	0.18	0.09	18.04	56.8	27.4	15.8
0.50-CS/CNT-8	332	0.27	0.09	11.37	52.3	23.5	24.2
0.50-CS/CNT-10	347	0.45	0.06	2.17	18.0	16.9	65.1

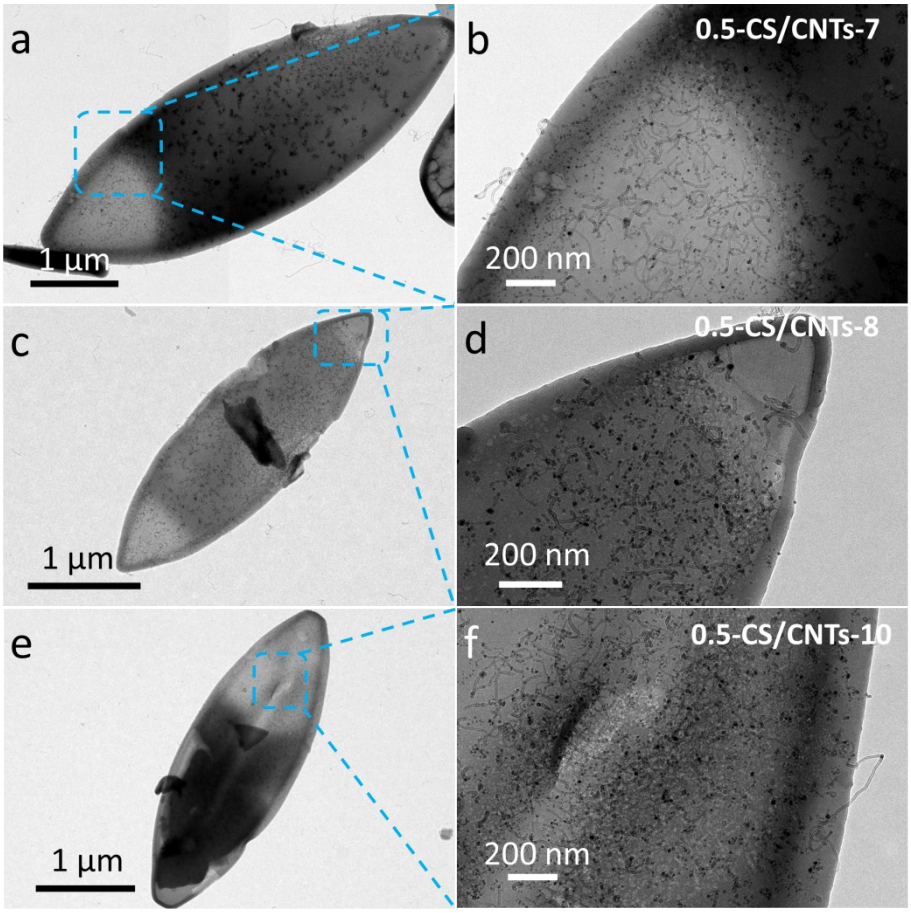

Fig. S4 The TEM (a, c and e) and enlarged TEM (b, d and f) images of 0.5-CS/CNTs-7, 0.5-CS/CNTs-8 and 0.5-CS/CNTs-10, respectively.

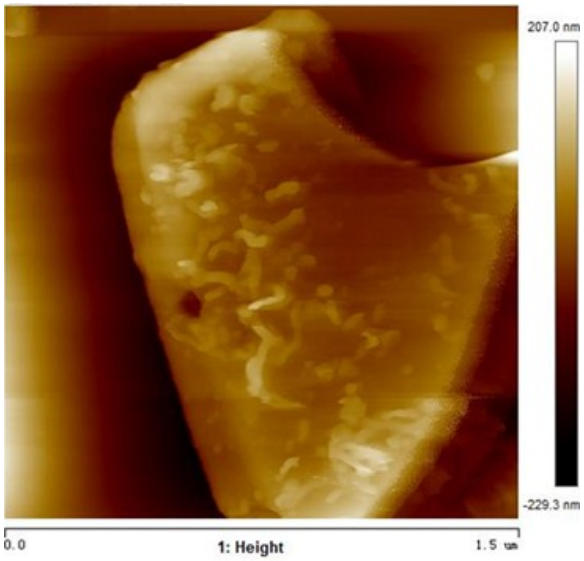

Fig. S5 The AFM image of 0.5-CS/CNTs-9.

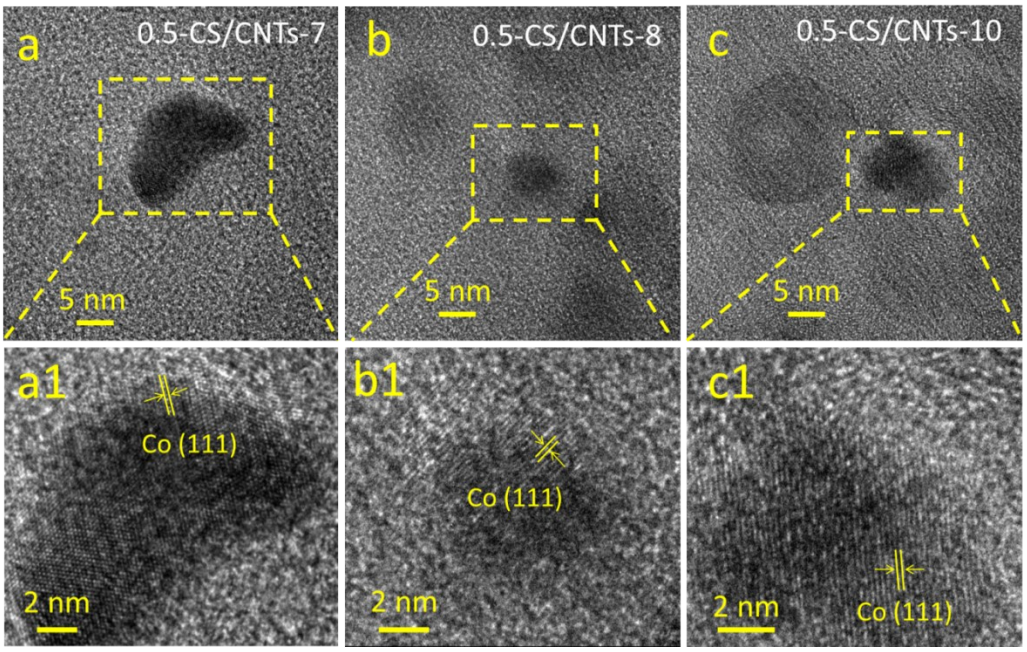

Fig. S6 The HR-TEM images of Co nanoparticle in 0.5-CS/CNT-7/8/10.

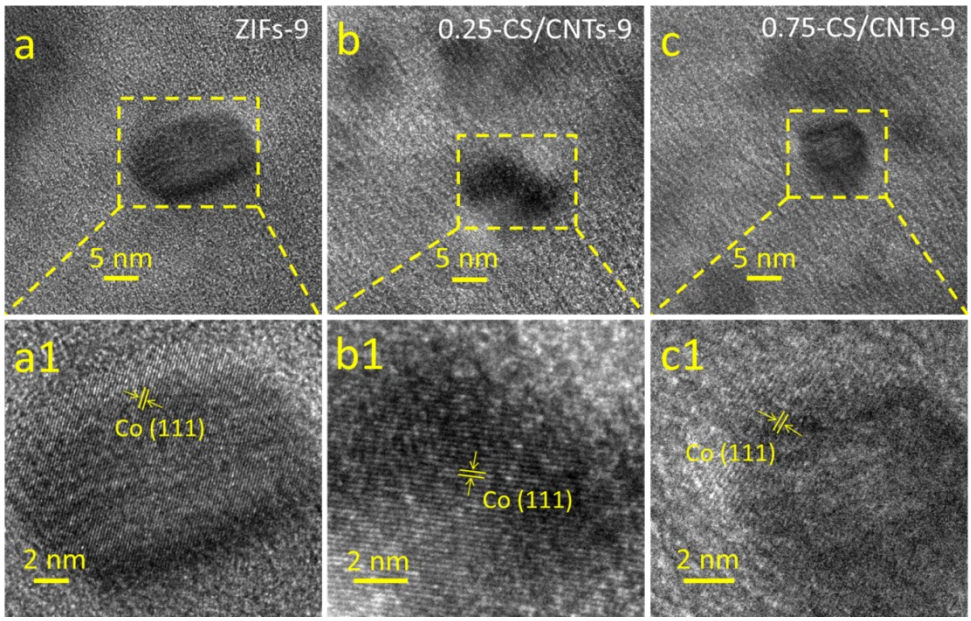

Fig. S7 The HR-TEM images of Co nanoparticle in ZIFs-9 and 0.25/0.75-CS/CNT-9.

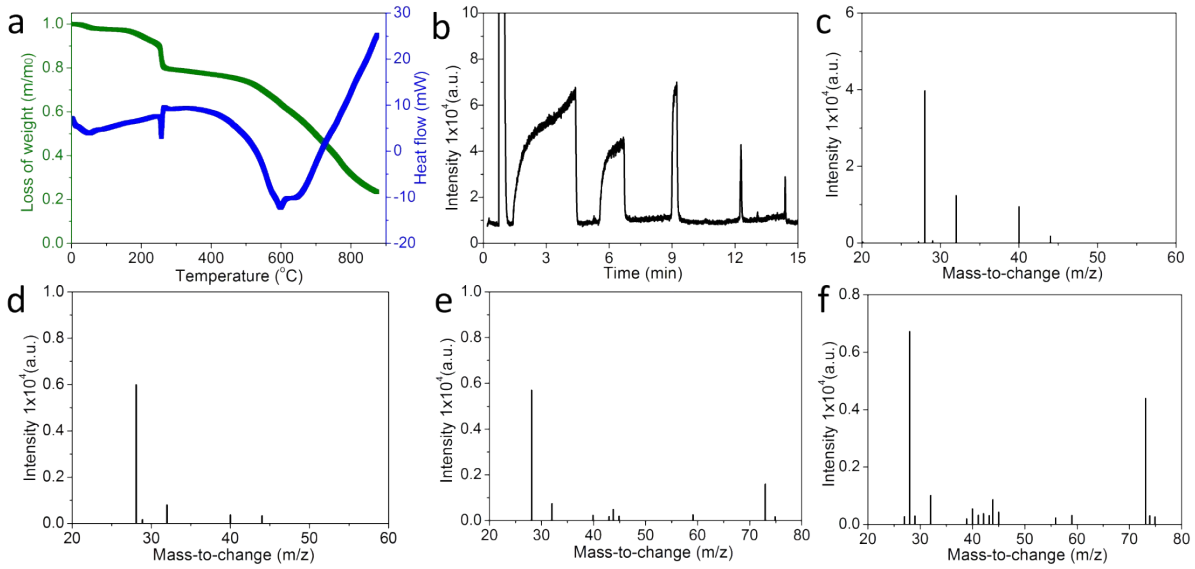

Fig. S8 (a) TGA and heat flow curves of 0.5-ZIFs@PDA in Ar atmosphere; the heating rate is 5 ˚C/min; (b-f) the GC spectrum and mass spectra of 0.5-ZIFs@PDA .

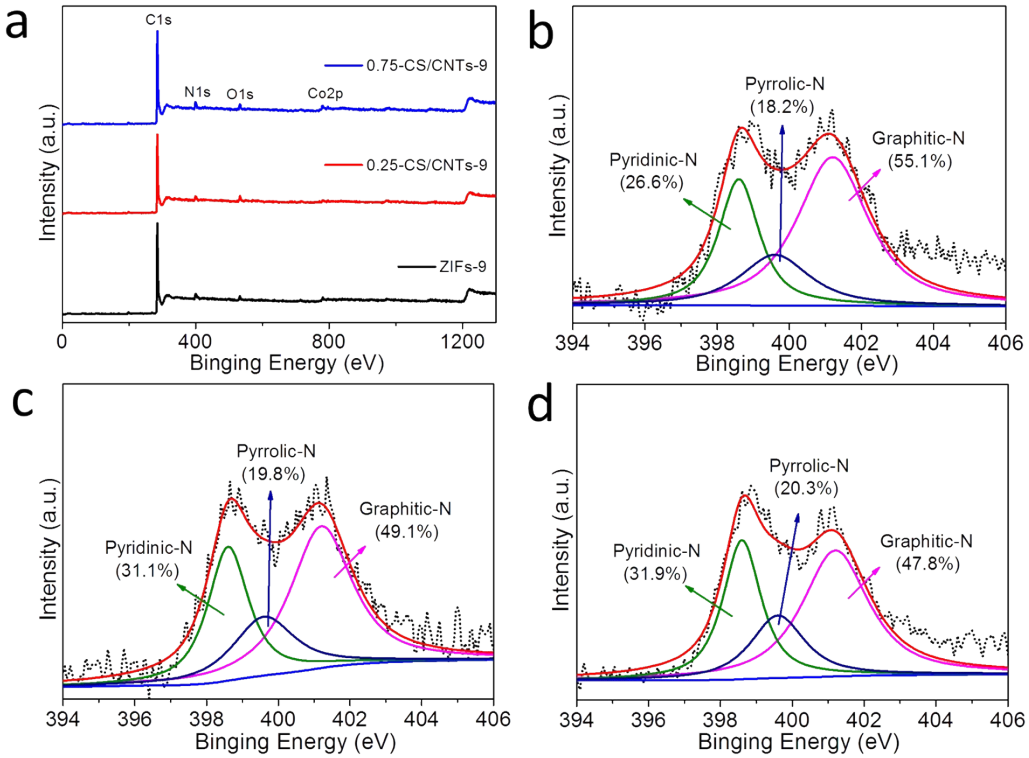

Fig. S9 The wide-range (a) and high-resolution N1s XPS spectra of 0.75-CS/CNTs-9 (b), 0.25-CS/CNTs-9 (c) and ZIFs-9 (d), respectively.

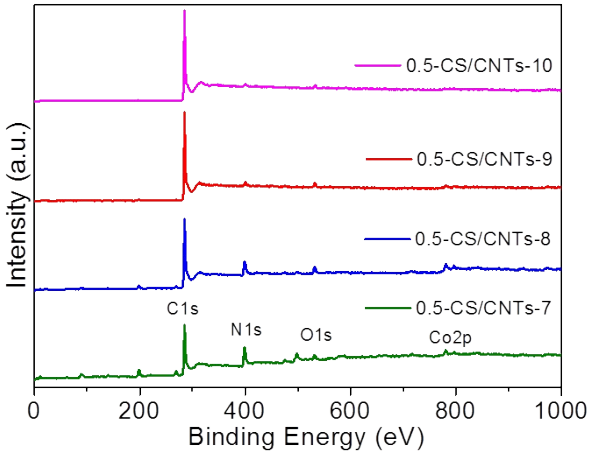

Fig. S10 The wide-range XPS spectra of 0.5-CS/CNTs-7, 0.5-CS/CNTs-8, 0.5-CS/CNTs-9, and 0.5-CS/CNTs-10.

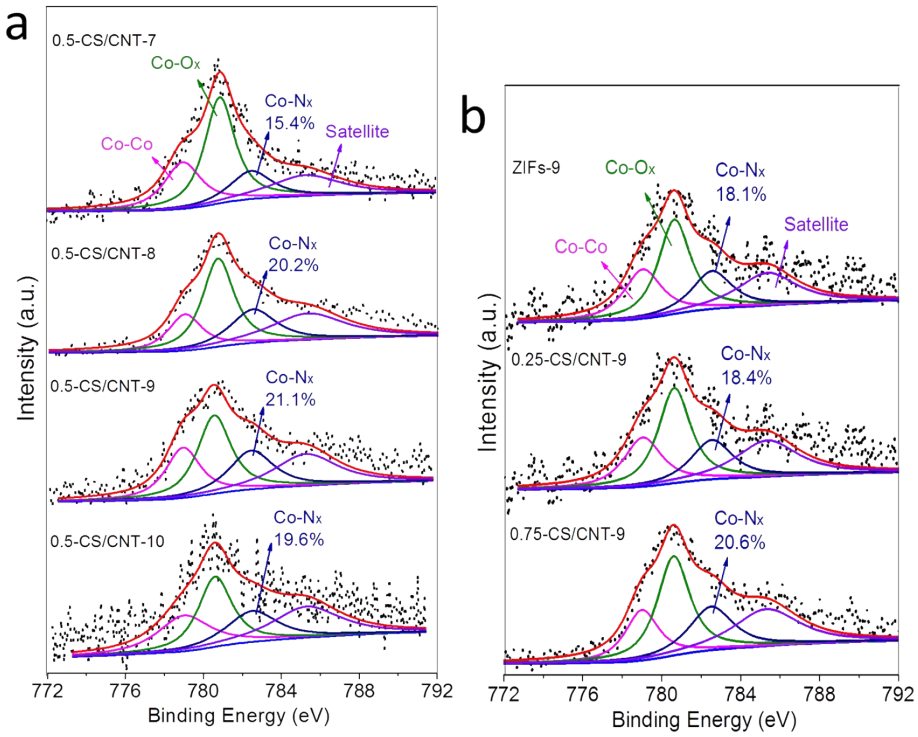

Fig S 11 high-resolution Co_{2p} XPS spectra of 0.5-CS/CNTs-7/8/9/10 (a) and ZIFs-9, 0.25/0.75-CS/CNTs-9 (b).

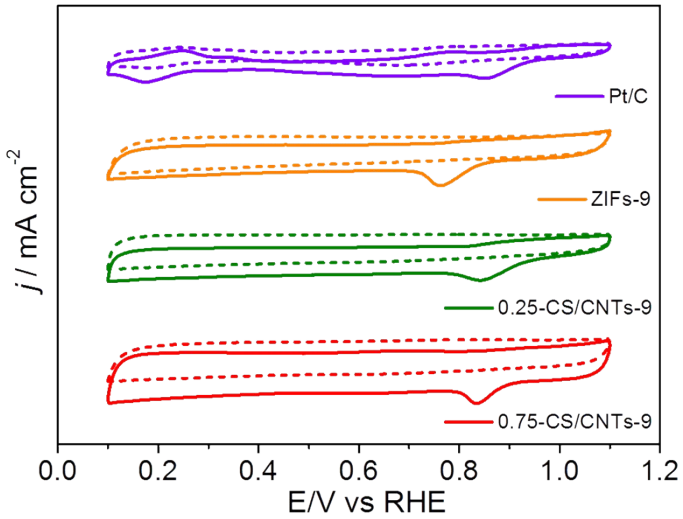

Fig. S12 CVs curves of Pt/C, ZIFs-9, 0.25-CS/CNTs-9 and 0.75-CS/CNTs-9 at a scan rate of 10 mV/s in N_2/O_2-saturated 0.1 M KOH solution

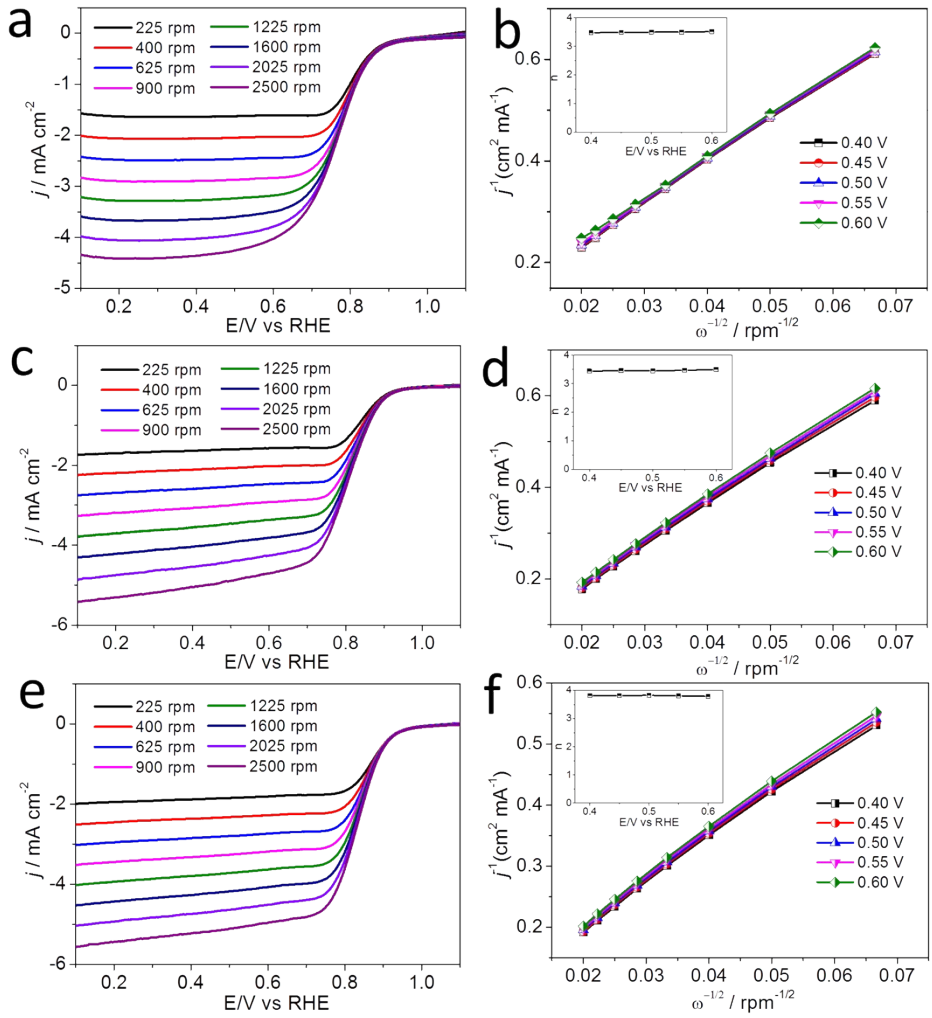

Fig. S13 The different rotation speeds of polarization curves (a, c and e) and K-L plots (b, d and f) of ZIFs-9, 0.25-CS/CNTs-9 and 0.75-CS/CNTs-9, respectively.

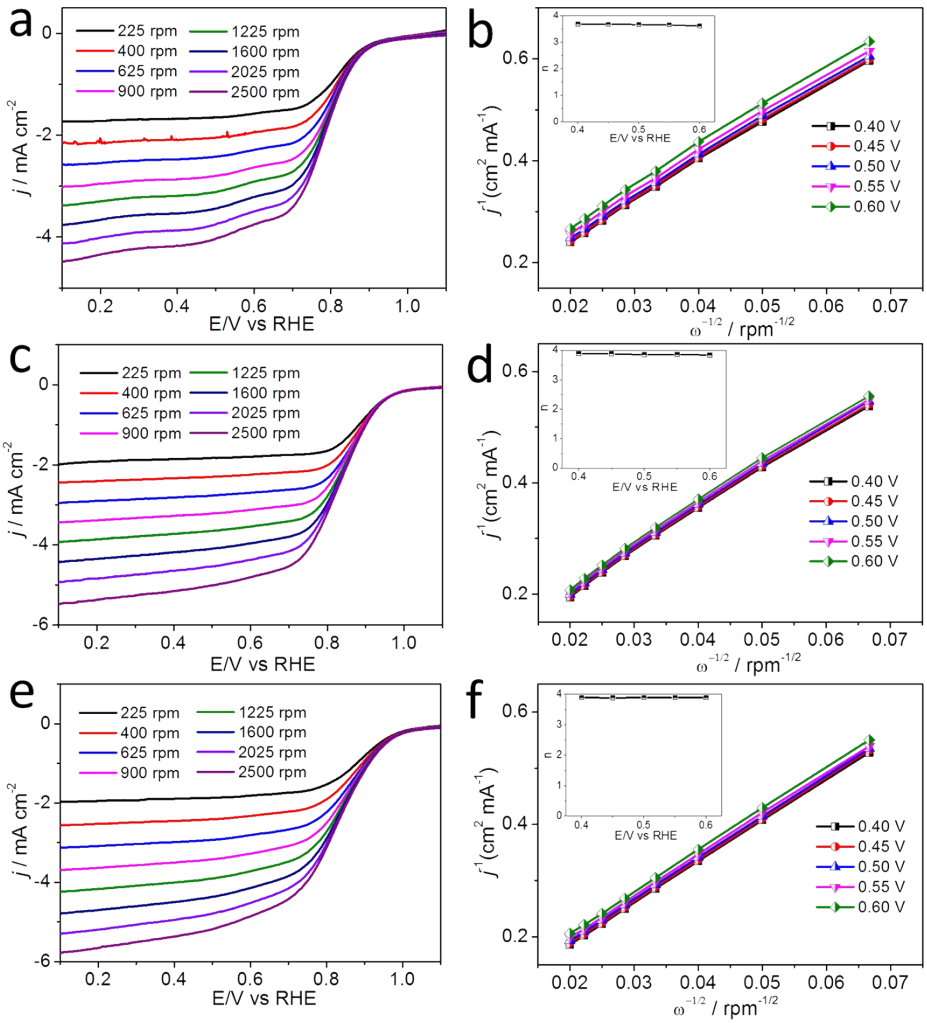

Fig. S14 The different rotation speeds of polarization curves (a, c and e) and K-L plots (b, d and f) of 0.5-CS/CNTs-7, 0.5-CS/CNTs-8 and 0.5-CS/CNTs-10, respectively.

Table. S2 the comparative of ORR performance.

Catalyst	**$E_{1/2}$ (V vs. Ag/AgCl) (Catalyst)**	**$E_{1/2}$ (V vs. Ag/AgCl) (Pt/C)**	**Ref.**
C-MOF-C2-900	0.817	0.815	1
GSP-1000	0.84	0.85	2
NixCoyO4/Co–NG	0.804	0.813	3
Co-N-C-0.4	0.84	0.84	4
N-CNTs-650	0.85	0.83	5
NC@Co-NGC DSNCs	0.81	0.82	6
Fe-N/C-800	0.851	0.868	7
0.5-CS/CNTs-9	0.857	0.861	This work

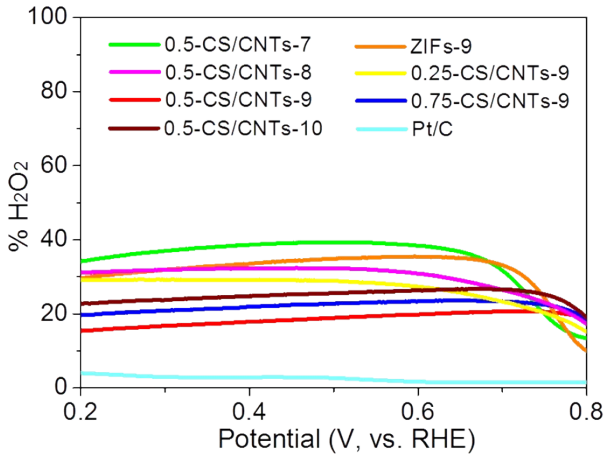

Fig. S15 H_2O_2 yield of Pt/C, ZIFs-9, 0.5-CS-CNTs-7/8/9/10 and 0.25/0.75-CS/CNTs-9 at various potentials based on RRDE data.

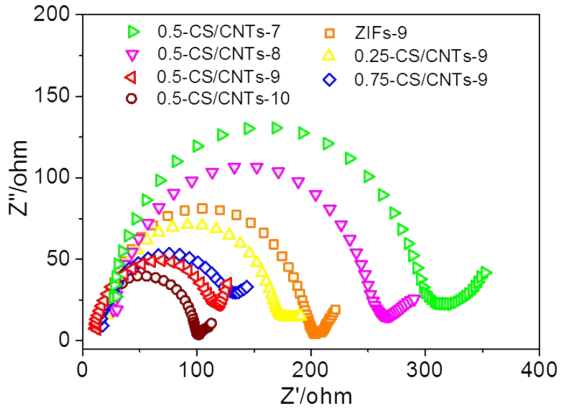

Fig. S16 Nyquist plots of 0.5-CS/CNTs-7/8/9/10, 0.25/0.75-CS/CNTs-9 and ZIFs-9 in the frequency range of 0.01-1000000 Hz.

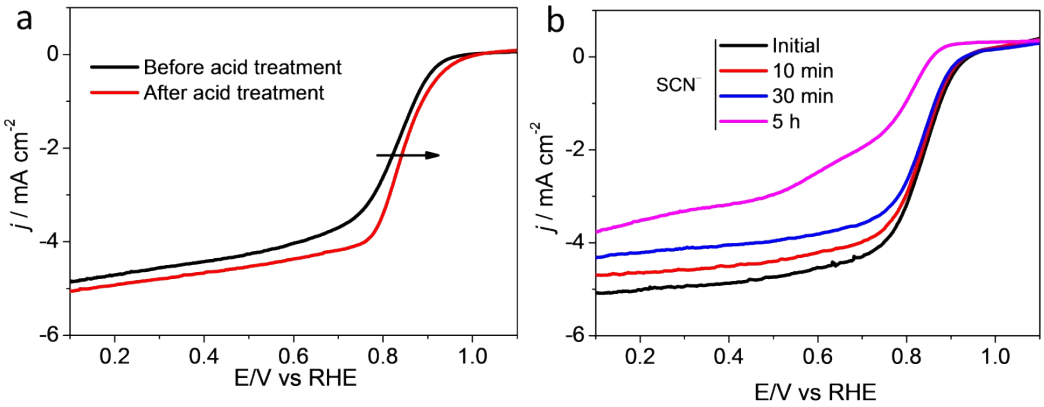

Fig. S17 (a) The LSV curves of as-prepared 0.5-CS/CNTs-9 before and after acid treatment; (b) effect of SCN^- ions on ORR performance.

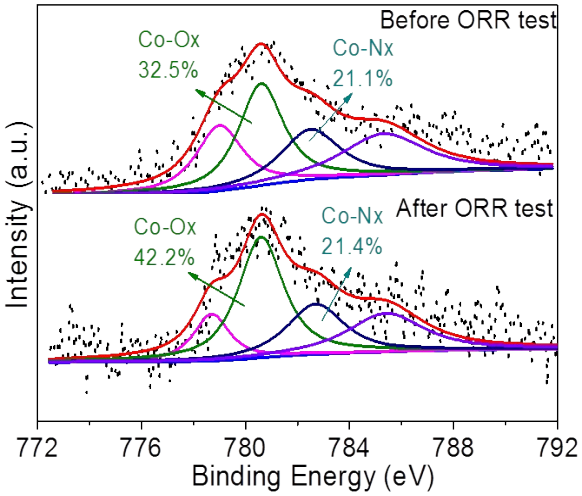

Fig. S18 The high-resolution Co_{2p} XPS spectra of 0.5-CS/CNTs-9 before and after ORR test.

References

1. M. Zhang, Q. Dai, H. Zheng, M. Chen and L. Dai, *Adv. Mater*., 2018, 1705431.

2. B. Huang, Y. Liu, X. Huang and Z. Xie. *J. Mater. Chem. A*, 2018, **6**, 22277.

3. Y. Hao, Y. Xu, J. Liu and X. Sun, *J. Mater. Chem. A*, 2017, **5**, 5594.

4. E. Hu, J. Ning, B. He, Z. Li, C. Zheng, Y. Zhong, Z. Zhang and Y. Hu, *J. Mater. Chem. A*, 2017, **5**, 2271.

5. J. Meng, C. Niu, L. Xu, J. Li, X. Liu, X. Wang, Y. Wu, X. Xu, W. Chen, Q. Li, Z. Zhu , D. Zhao and L. Mai, *J. Am. Chem. Soc*., 2017, **139**, 8212.

6. S. Liu, Z. Wang, S. Zhou, F. Yu, M. Yu, C. Y. Chiang, W. Zhou, J. Zhao and J. Qiu, *Adv. Mater*., 2017, 1700874.

7. L. Lin, Q. Zhu, and A. -W. Xu, *J. Am. Chem. Soc*. 2014, **136**, 11027.